PHYSICAL REVIEW A **66**, 061601(R) (2002)

Spinor Bose-Einstein condensates with many vortices

T. Kita,[1] T. Mizushima,[2] and K. Machida[2]
[1]*Division of Physics, Hokkaido University, Sapporo 060-0810, Japan*
[2]*Department of Physics, Okayama University, Okayama 700-8530, Japan*
(Received 31 March 2002; published 18 December 2002)

Vortex-lattice structures of antiferromagnetic spinor Bose-Einstein condensates with hyperfine spin $F=1$ are investigated theoretically based on the Ginzburg-Pitaevskii equations near T_c. The Abrikosov lattice with clear core regions is never found to be stable at any rotation drive Ω. Instead, each component Ψ_i $(i=0,\pm1)$ prefers to shift the core locations away from the others to realize almost uniform order-parameter amplitude with complicated magnetic-moment configurations. This system is characterized by many competing metastable structures so that quite a variety of vortices may be realized with a small change in external parameters.

DOI: 10.1103/PhysRevA.66.061601 PACS number(s): 03.75.Fi, 05.30.Jp

Manipulating various experimental techniques, several groups have succeeded recently in creating quantized vortices in the Bose-Einstein condensates (BEC's) of atomic gases [1–4]. Especially interesting in these systems are vortices of spinor BEC's in optically trapped ^{23}Na [5] and ^{87}Rb [6], where new physics absent in superconductors [7], ^{4}He [8], and ^{3}He [9–11], may be found.

Theoretical investigations on spinor BEC's were started by Ohmi and Machida [12] and Ho [13], followed by detailed studies on vortices with a single circulation quantum [14–23]. However, no calculations have been performed yet on structures in rapid rotation where the trap potential will play a less important role. Indeed, the clear hexagonal-lattice image of magnetically trapped ^{23}Na [3] suggests that predictions on infinite systems are more appropriate for BEC's with many vortices. Such calculations have been carried out by Ho for the single-component BEC [24] and by Mueller and Ho for a two-component BEC [25] near the upper critical angular velocity Ω_{c2} at $T=0$.

The purpose of the present paper is to perform detailed calculations on vortices of $F=1$ spinor BEC's in rapid rotation to clarify their essential features. To this end, we focus on the mean-field high-density phase rather than the low-density correlated liquid phase [26], and use the phenomenological Ginzburg-Pitaevskii (or Ginzburg-Landau) equations near T_c [27,28] instead of the Gross-Pitaevskii equations at $T=0$. Since fluctuations are small in the present system, this approach will yield quantitatively correct results near T_c. It should be noted that the corresponding free energy is formally equivalent to that derived with Ho's ''mean-field quantum Hall regime'' near Ω_{c2} at $T=0$ [24,25], so that the results obtained here are also applicable to that region.

Model. The free-energy density of an $F=1$ spinor BEC near T_c may be expanded with respect to the order parameters Ψ_i $(i=0,\pm1)$ as

$$f=-\alpha\Psi_i^*\Psi_i+\Psi_i^*\frac{(-i\hbar\nabla-M\mathbf{\Omega}\times\mathbf{r})^2}{2M}\Psi_i + \frac{\beta_n}{2}\Psi_i^*\Psi_j^*\Psi_i\Psi_j+\frac{\beta_s}{2}\Psi_i^*\Psi_j^*(F_\mu)_{ik}(F_\mu)_{jl}\Psi_k\Psi_l. \tag{1}$$

Here α, β_n, and β_s are expansion parameters, F_μ $(\mu=x,y,z)$ denotes the spin operator, M is the particle mass, and summations over repeated indices are implied. The rotation axis $\mathbf{\Omega}$ is taken along $\mathbf{z}$. The quantities β_n and β_s are assumed to be constant near T_c with $\beta_n>0$, whereas α changes its sign at T_c with $\alpha>0$ for $T<T_c$. To simplify Eq. (1), we measure the length, the energy density, the angular velocity, and the order parameter in units of $\hbar/\sqrt{2M\alpha}$, α^2/β_n, $\alpha/\hbar$, and α/β_n, respectively. The corresponding free-energy density is obtained from Eq. (1) by $\alpha\to1$, $\beta_n\to1$, $\hbar^2/2M\to1$, $M\mathbf{\Omega}\to\frac{1}{2}\mathbf{\Omega}$, and $\beta_s\to g_s\equiv\beta_s/\beta_n$. It thus takes a simple form with only two parameters (g_s,Ω). We then introduce a couple of operators by $a\equiv\ell(\partial_x+i\partial_y)/\sqrt{2}$ and $a^\dagger\equiv\ell(-\partial_x+i\partial_y)/\sqrt{2}$ with $\boldsymbol{\partial}\equiv\nabla-i/2\mathbf{\Omega}\times\mathbf{r}$ and $\ell\equiv1/\sqrt{\Omega}$, which satisfy $aa^\dagger-a^\dagger a=1$. Equation (1) now reads

$$f=\Psi_i^*[(2a^\dagger a+1)\Omega-1]\Psi_i+\frac{1}{2}\Psi_i^*\Psi_j^*\Psi_i\Psi_j + \frac{g_s}{2}\Psi_i^*\Psi_j^*(F_\mu)_{ik}(F_\mu)_{jl}\Psi_k\Psi_l, \tag{2}$$

and the free energy is given by

$$\mathcal{F}\equiv\int f(\mathbf{r})d\mathbf{r}. \tag{3}$$

We can find the stable structure for each (g_s,Ω) by minimizing $\mathcal{F}$; it is easily seen that Ψ_i becomes finite below $\Omega_{c2}=1$. We have performed extensive calculations over the whole antiferromagnetic region $g_s\geqslant0$, where $(\Psi_1,\Psi_0,\Psi_{-1})=e^{i\theta}\mathcal{U}(0,1,0)$ and $f=\frac{1}{2}$ at $\Omega=0$ with θ an arbitrary phase and $\mathcal{U}$ the spin-space rotation [13].

A major difference from superfluid ^{3}He [11] lies in the fact that terms such as $\Psi_i^*aa\Psi_j$ $(i\neq j)$ are absent, i.e., there are no gradient couplings between different components. Hence Ω_{c2} is the same for all components, whereas in ^{3}He only a single component becomes finite at Ω_{c2} to realize the polar state [11]. This degenerate feature is what characterizes the present system to bring many competing metastable structures, as seen below.

Method. We minimize Eq. (3) with the Landau-level-expansion method (LLX) [11,29] by expanding the order parameters as

$$\Psi_i(\mathbf{r}) = \sqrt{\mathcal{V}} \sum_{N=0}^{\infty} \sum_{\mathbf{q}} c_{N\mathbf{q}}^{(i)} \psi_{N\mathbf{q}}(\mathbf{r}), \tag{4}$$

with N the Landau-level index, $\mathbf{q}$ the magnetic Bloch vector, and $\mathcal{V}$ the system volume. The basis functions $\{\psi_{N\mathbf{q}}\}$ are eigenstates of the magnetic translation operator $T_{\mathbf{R}} \equiv \exp[-\mathbf{R}\cdot(\boldsymbol{\nabla} + i/2\boldsymbol{\Omega}\times\mathbf{r})]$, where $\mathbf{R}$ denotes a lattice point spanned by two basic vectors $\mathbf{a}_1 \equiv (a_{1x}, a_{1y}, 0)$ and $\mathbf{a}_2 \equiv (0, a_2, 0)$ satisfying $a_{1x}a_2 = 2\pi\ell^2$. Thus, every basic cell holds a unit circulation quantum $\kappa \equiv h/M$, and $\mathbf{q}$ runs in the Brillouin zone spanned by two basic vectors $\mathbf{b}_1 \equiv \mathbf{a}_2 \times \hat{\mathbf{z}}/\ell^2$ and $\mathbf{b}_2 \equiv \hat{\mathbf{z}} \times \mathbf{a}_1/\ell^2$ of the reciprocal lattice. This $\{\psi_{N\mathbf{q}}\}$ can describe all the periodic vortex structures [29], whose explicit expression is given by

$$\begin{aligned}\psi_{N\mathbf{q}}(\mathbf{r}) = & \sum_{n=-\mathcal{N}_f/2+1}^{\mathcal{N}_f/2} e^{i[q_y(y+\ell^2 q_x/2) + n a_{1x}(y+\ell^2 q_x - n a_{1y}/2)/\ell^2]} \\ & \times e^{-ixy/2\ell^2 - (x-\ell^2 q_y - n a_{1x})^2/2\ell^2} \\ & \times \sqrt{\frac{2\pi\ell/a_2}{2^N N!\sqrt{\pi}\mathcal{V}}} H_N\left(\frac{x-\ell^2 q_y - n a_{1x}}{\ell}\right),\end{aligned} \tag{5}$$

with $\mathcal{N}_f^2$ denoting the number of κ's in the system and H_N the Hermite polynomial. We substitute Eq. (4) into Eq. (3), make a change of variables as $(x,y) = (a_{1x}s, a_{1y}s + a_2 t)$, and carry out the integration with respect to (s,t). Then Eq. (3) is transformed into a functional of the expansion coefficients $\{c_{N\mathbf{q}}^{(i)}\}$, the apex angle $\beta \equiv \cos^{-1}(a_{1y}/a_1)$, and the ratio of the two basic vectors $\rho \equiv a_2/a_1$ as $\mathcal{F} = \mathcal{F}[\{c_{N\mathbf{q}}^{(i)}\}, \beta, \rho]$. For a given Ω, we directly minimize $\mathcal{F}/\mathcal{V}$ with respect to these quantities.

Search for stable structures. We here sketch our strategy to find stable structures. To this end, we first summarize the basic features of the conventional Abrikosov lattice within the framework of LLX [29]: (i) any single $\mathbf{q} = \mathbf{q}_1$ suffices, due to the broken translational symmetry of the vortex lattice; (ii) the triangular (square) lattice is made up of $N = 6n$ $(4n)$ Landau levels $(n = 0,1,2,\ldots)$; (iii) more general structures can be described by $N = 2n$ levels, odd N's never mixing up since those bases have finite amplitudes at the cores. This Abrikosov lattice has a single circulation quantum per unit cell.

With multicomponent order parameters, there can be a wide variety of vortices, which may be divided into two categories. We call the first category as ''shift-core'' states, where core locations are different among the three components with an enlarged unit cell. General structures with n_κ circulation quanta per unit cell can be described by using n_κ different $\mathbf{q}$'s, where the unit cell becomes n_κ times as large as that of the Abrikosov lattice. For example, structures with two quanta per unit cell are given by choosing $(\mathbf{q}_1, \mathbf{q}_2) = [\mathbf{0}, (\mathbf{b}_1 + \mathbf{b}_2)/2]$. This possibility was already considered by Mueller and Ho [25] for a two-component system and shown to yield stable structures. It also describes the mixed-twist lattice to be found in ^{3}He [11]. The second category may be called ''fill-core'' states with a single circulation quantum per unit cell (i.e., a single $\mathbf{q}$ is relevant). Here the cores of the conventional Abrikosov lattice are filled in by some superfluid components using odd-N wave functions of Eq. (5). This entry of odd-N Landau levels occurs as a second-order transition below some critical angular velocity smaller than $\Omega_{c2}/3$. It has been shown that the A-phase-core vortex in the B phase of superfluid ^{3}He belongs to this category [11].

We have carried out an extensive search for stable structures with up to $n_\kappa = 9$ circulation quanta per unit cell, including fill-core states. Since we are near T_c where normal particles are also present, we have performed the minimization without specifying the value of the magnetic moment M for the superfluid components. However, all the stable states found below have $M = 0$. Each of the three components were expanded as Eq. (4) using n_κ different $\mathbf{q}$'s, and the free energy (3) is minimized with respect to $c_{N\mathbf{q}}^{(i)}$, β, and ρ by using Powell's method [30]. To pick out stable structures correctly, we calculated Eq. (3) many times starting from different initial values for $c_{0\mathbf{q}}^{(i)}$, β, and ρ given randomly within $0.1 \leqslant \mathrm{Re}c_{0\mathbf{q}}^{(i)}$, $\mathrm{Im}c_{0\mathbf{q}}^{(i)} \leqslant 0.9$, $0.1\pi \leqslant \beta \leqslant 0.5\pi$, and $0.8 \leqslant \rho \leqslant 3$, respectively. The state with the lowest energy was thereby identified as the stable structure. The spin quantization axis and an overall phase were fixed conveniently to perform efficient calculations. Thus, any structures obtained from the solutions below with a spin-space rotation and a gauge transformation are also stable.

Instability of the Abrikosov lattice. The present calculations have revealed that the Abrikosov lattice with clear core regions is never stable at any rotation drive Ω over the entire antiferromagnetic region $g_s \geqslant 0$. Thus, any optical experiments to detect vortices by amplitude reductions are not suitable for the spinor vortices.

The lowest-energy Abrikosov lattice is given by

$$\Psi_0(\mathbf{r}) = \sqrt{V} \sum_N c_N^{(0)} \psi_{N\mathbf{q}_1}(\mathbf{r}), \tag{6}$$

with $c_{N\mathbf{q}_1}^{(0)}$ real, $N = 6n$, $\beta = \pi/3$, and $\rho = 1$. Here the antiferromagnetic component Ψ_0 forms a hexagonal lattice with a single circulation quantum per unit cell. Below some critical velocity Ω_f smaller than $\Omega_{c2}/3$, the core regions start to be filled in by

$$\Psi_{\pm 1}(\mathbf{r}) = i\sqrt{V} \sum_{N'} c_{N'}^{(1)} \psi_{N'\mathbf{q}_1}(\mathbf{r}), \tag{7}$$

with N' odd. The second transition for this odd-Landau-level entry occurs at $\Omega_f = 0.1497\Omega_{c2}$ and $0.0938\Omega_{c2}$ for $g_s = 0.1$ and 0.3, respectively.

However, calculations down to $0.0001\Omega_{c2}$ of using 1800 Landau levels for $g_s \geqslant 0$ have clarified that the above fill-core state carries higher free energy than the following shift-core state with two circulation quanta per unit cell:

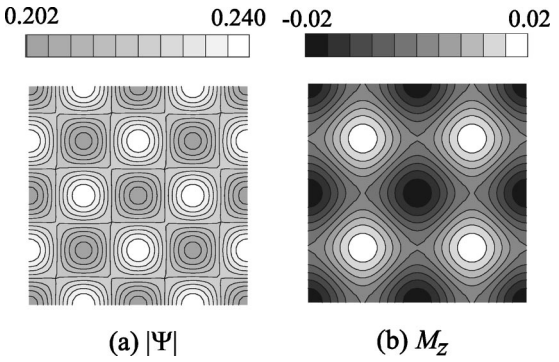

FIG. 1. Spatial variations of (a) the order-parameter amplitude and (b) the magnetic moment along z, for the shift-core state (8), (9) over $|x|,|y| \leqslant a_1$ at $g_s=0.08$ and $\Omega=0.95\Omega_{c2}$. The moment is directed along **z**.

$$\Psi_1(\mathbf{r}) = \sqrt{V} \sum_N c_N \psi_{N\mathbf{q}_1}(\mathbf{r}), \tag{8}$$

$$\Psi_{-1}(\mathbf{r}) = \sqrt{V} \sum_N c_N \psi_{N\mathbf{q}_2}(\mathbf{r}), \tag{9}$$

with c_N real and common to both, $N=4n$, $\beta=\pi/2$, $\rho=1$, and $(\mathbf{q}_1,\mathbf{q}_2)=[\mathbf{0},(\mathbf{b}_1+\mathbf{b}_2)/2]$. The cores of $\Psi_{\pm 1}(\mathbf{r})$ are shifted from each other by $\frac{1}{2}(\mathbf{a}_1+\mathbf{a}_2)$. Figure 1 displays basic features of this shift-core state. The order-parameter amplitude $|\Psi|$ is almost uniform, and the magnetic moment M_z is ordered antiferromagnetically along z axis. This moment M_z is seen to vanish at points where $|\Psi|$ takes its maximum value; there the bulk order-parameter configuration $(\Psi_1,\Psi_0,\Psi_{-1}) \propto e^{i\theta}\mathcal{U}(0,1,0)$ is realized.

Stable structures at $\Omega=0.95\Omega_{c2}$. Having seen that the conventional Abrikosov lattice is never favored in the whole antiferromagnetic domain $g_s \geqslant 0$, we now enumerate all the stable structures found at $\Omega=0.95\Omega_{c2}$ to clarify their essential features. This rapidly rotating domain is especially interesting, because the same free energy also becomes relevant near Ω_{c2} at $T=0$, as shown by Ho using a "mean-field quantum Hall regime" [24]. Thus, the conclusions obtained here are also applicable to the region at $T=0$.

Figure 2 displays the lowest free energy per unit volume as a function of g_s for $\Omega=0.95\Omega_{c2}$. The value of each n_κ denotes the number of circulation quanta per unit cell. A special feature to be noted is that these various structures are energetically quite close to each other; for example, the $n_\kappa=8$ state at $g_s=0.02$ is favored over the $n_\kappa=3$ state by a relative free-energy difference of order 10^{-6}. This fact suggests that we may realize quite a variety of metastable structures by a small change of the boundary conditions, the rotation process, etc.

Details of these structures are summarized as follows.

The $n_\kappa=2$ state of Eqs. (8) and (9) is stable for $g_s \geqslant 0.0671$. We have already seen its basic features above.

The $n_\kappa=3,5,7$ states can be expressed compactly as

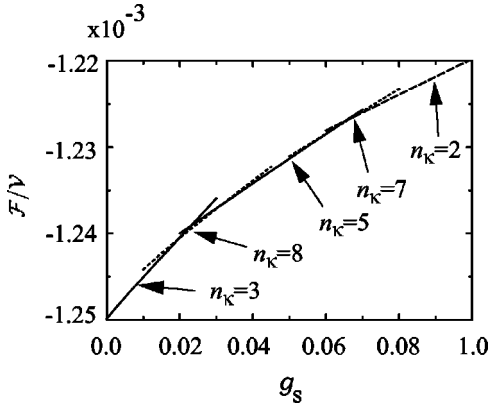

FIG. 2. Calculated free energy per unit volume as a function of g_s at $\Omega=0.95\Omega_{c2}$. Five different structures have been found for $g_s \geqslant 0$, and the value of each n_κ denotes the number of circulation quanta per unit cell for each stable structure.

$$\Psi_0 = \sum_N \sum_{\nu=1}^{(n_\kappa-1)/2} c^{(0)}_{N\mathbf{q}_\nu} (\psi_{N\mathbf{q}_\nu} - e^{-2i(\nu/n_\kappa)\pi} \psi_{N\mathbf{q}_{n_\kappa-\nu}}), \tag{10}$$

$$\Psi_{\pm 1} = \sum_N \left[\sum_{\nu=1}^{(n_\kappa-1)/2} c^{(\pm 1)}_{N\mathbf{q}_\nu} (\psi_{N\mathbf{q}_\nu} + e^{-2i(\nu/n_\kappa)\pi} \psi_{N\mathbf{q}_{n_\kappa-\nu}}) + c^{(\pm 1)}_{N\mathbf{q}_{n_\kappa}} \psi_{N\mathbf{q}_{n_\kappa}} \right], \tag{11}$$

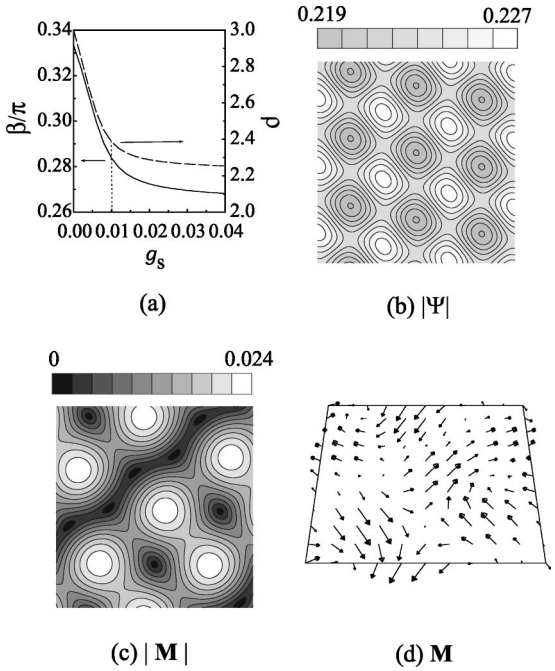

FIG. 3. (a) Variations of β/π and ρ as a function of g_s for the $n_\kappa=3$ state at $\Omega=0.95\Omega_{c2}$. This lattice for $g_s=0$ is hexagonal with $\beta=\pi/3$ and $\rho=3$. (b)–(d) display, for $g_s=0.01$, spatial variations of (b) the order-parameter amplitude, (c) amplitude of the magnetic moment, and (d) the magnetic moment, over $-3a_{1x}/2 < x < 3a_{1x}/2$ and $-a_2/2 < y < a_2/2$.

where N's are even and $\mathbf{q}_\nu=(\nu/n_\kappa)\mathbf{b}_1$. These $n_\kappa=3,5,7$ states are stable for $0\leqslant g_s\leqslant 0.0196$, $0.0313\leqslant g_s\leqslant 0.0613$, and $0.0613\leqslant g_s\leqslant 0.0671$, respectively. Unlike the two component system considered by Mueller and Ho [25] where each component is specified by a single-$\mathbf{q}$ basis function, Ψ_m here is made up of multiple basis functions $\psi_{N\mathbf{q}_\nu}$ whose cores are shifted from each other by $(\nu/n_\kappa)\mathbf{a}_2$. Figure 3 displays the basic features of the $n_\kappa=3$ state. The lattice is hexagonal at $g_s=0$, but deforms rapidly as g_s increases. The order-parameter amplitude is again almost constant, and the magnetic moment $\mathbf{M}$ has a complicated structure. These features are common to all the $n_\kappa\geqslant 3$ states discussed here, although no details are presented for the other states. The lattice parameters (β,ρ) for $n_\kappa=5,7$ states are $(0.1311\pi,2.056)$ and $(0.1830\pi,2.609)$ for $g_s=0.05$ and 0.066, respectively, which change little in each relevant range of stability.

The remaining $n_\kappa=8$ state, stable over $0.0196\leqslant g_s\leqslant 0.0313$, is given by

$$\Psi_0=\sum_N c^{(0)}_{N\mathbf{q}_1}(\psi_{N\mathbf{q}_1}+\psi_{N\mathbf{q}_2}-\psi_{N\mathbf{q}_3}+i\psi_{N\mathbf{q}_4}), \tag{12}$$

$$\Psi_{\pm 1}=\sum_N\sum_{\nu=5}^{8} c^{(\pm 1)}_{N\mathbf{q}_\nu}\psi_{N\mathbf{q}_\nu}, \tag{13}$$

where $\mathbf{q}_1=(\mathbf{b}_1+\mathbf{b}_2)/2$, $\mathbf{q}_2=\mathbf{0}$, $\mathbf{q}_3=(\mathbf{b}_1-\mathbf{b}_2)/4$, $\mathbf{q}_4=c-(\mathbf{b}_1+\mathbf{b}_2)/4$, $\mathbf{q}_5=(\mathbf{b}_1)/2$, $\mathbf{q}_6=\mathbf{b}_2/2$, $\mathbf{q}_7=(\mathbf{b}_1+\mathbf{b}_2)/4$, and $\mathbf{q}_8=-(\mathbf{b}_1-\mathbf{b}_2)/4$. The parameters (β,ρ) at $g_s=0.025$ are $(0.3317\pi,1.049)$, and changes only slightly in the above range of g_s.

Concluding remarks. We have performed extensive calculations on antiferromagnetic $F=1$ spinor vortices in rapid rotation. The conventional Abrikosov lattice is shown to be never favored. Each stable structure has almost constant order-parameter amplitude and a complicated magnetic-moment configuration, as shown in Figs. 1 and 3, for example. This means that any optical experiments to detect vortices by amplitude reduction will not be suitable for the spinor vortices. Instead, techniques to directly capture spatial magnetic-moment configurations will be required. The system has many metastable structures that are different in the number of circulation quanta per unit cell n_κ, but are quite close to each other energetically. Thus, domains to separate different structures may be produced easily. This degenerate feature is also present within the (β,ρ) space of a fixed n_κ, where β is the vortex-lattice apex angle and ρ is the length ratio of the two basic vectors. Putting it differently, we can deform a stable lattice structure with a tiny cost of energy. These facts indicate that the spinor BEC's can be a rich source of novel vortices realized with a small change in external parameters. To observe those states, however, one would presumably need a very high stability of the experimental setup, because the small energy differences may also make them less robust to noise.

This research was supported by a Grant-in-Aid for Scientific Research from the Ministry of Education, Culture, Sports, Science, and Technology of Japan.

[1] M.R. Matthews, B.P. Anderson, P.C. Haljan, D.S. Hall, C.E. Wieman, and E.A. Cornell, Phys. Rev. Lett. **83**, 2498 (1999).
[2] K.W. Madison, F. Chevy, W. Wohlleben, and J. Dalibard, Phys. Rev. Lett. **84**, 806 (2000).
[3] J.R. Abo-Shaeer, C. Raman, J.M. Vogels, and W. Ketterle, Science **292**, 476 (2001).
[4] P.C. Haljan, I. Coddington, P. Engels, and E.A. Cornell, Phys. Rev. Lett. **87**, 210403 (2001).
[5] J. Stenger, S. Inouye, D.M. Stamper-Kurn, H.-J. Miesner, A.P. Chikkatur, and W. Ketterle, Nature (London) **369**, 345 (1998).
[6] M.D. Barrett, J.A. Sauer, and M.S. Chapman, Phys. Rev. Lett. **87**, 010404 (2001).
[7] See, e. g., M. Tinkham, *Introduction to Superconductivity* (McGraw-Hill, New York, 1996).
[8] R.J. Donnelly, *Quantized Vortices in Helium II* (Cambridge University Press, Cambridge, 1991).
[9] M.M. Salomaa and G.E. Volovik, Rev. Mod. Phys. **59**, 533 (1987).
[10] O.V. Lounasmaa and E. Thuneberg, Proc. Natl. Acad. Sci. U.S.A. **96**, 7760 (1999).
[11] T. Kita, Phys. Rev. Lett. **86**, 834 (2001).
[12] T. Ohmi and K. Machida, J. Phys. Soc. Jpn. **67**, 1822 (1998).
[13] T.-L. Ho, Phys. Rev. Lett. **81**, 742 (1998).
[14] S.K. Yip, Phys. Rev. Lett. **83**, 4677 (1999).
[15] Th. Busch and J.R. Anglin, Phys. Rev. A **60**, R2669 (1999).
[16] U. Leonhardt and G.E. Volovik, JETP Lett. **72**, 46 (2000).
[17] K.-P. Marzlin, W. Zhang, and B.C. Sanders, Phys. Rev. A **62**, 013602 (2000).
[18] U.A. Khawaja and H.T.C. Stoof, Nature (London) **411**, 918 (2001); Phys. Rev. A **64**, 043612 (2001).
[19] J.-P. Martikainen, A. Collin, and K.-A. Suominen, e-print cond-mat/0106301.
[20] S. Tuchiya and S. Kurihara, J. Phys. Soc. Jpn. **70**, 1182 (2001).
[21] T. Isoshima, K. Machida, and T. Ohmi, J. Phys. Soc. Jpn. **70**, 1604 (2001).
[22] T. Isoshima and K. Machida, e-print cond-mat/0201507.
[23] T. Mizushima, K. Machida, and T. Kita, e-print cond-mat/0203242.
[24] T.-L. Ho, Phys. Rev. Lett. **87**, 060403 (2001).
[25] E.J. Mueller and T.-L. Ho, e-print cond-mat/0201051.
[26] N.R. Cooper, N.K. Wilkin, and J.M.F. Gunn, Phys. Rev. Lett. **87**, 120405 (2001).
[27] V.L. Ginzburg and L.P. Pitaevskii, Zh. Éksp. Teor. Fiz. **34**, 1240 (1958) [Sov. Phys. JETP **7**, 858 (1958)].
[28] For a review on this approach, see, V.L. Ginzburg and A.A. Sobyanin, J. Low Temp. Phys. **49**, 507 (1982).
[29] T. Kita, J. Phys. Soc. Jpn. **67**, 2067 (1998).
[30] W.H. Press, S.A. Teukolsky, W.T. Vetterling, and B.P. Flannery, *Numerical Recipes in C* (Cambridge University Press, Cambridge, 1988).